ChemBioChem

Research Article
doi.org/10.1002/cbic.202300453

Chemistry Europe
European Chemical Societies Publishing

www.chembiochem.org

Exploring Photoswitchable Binding Interactions with Small-Molecule- and Peptide-Based Inhibitors of Trypsin

Kathryn A. Palasis,[a] Victoria Peddie,[a] Dion J. L. Turner,[a] Xiaozhou Zhang,[a] Jingxian Yu,[a, b] and Andrew D. Abell*[a]

The ability to photochemically activate a drug, both when and where needed, requires optimisation of the difference in biological activity between each isomeric state. As a step to this goal, we report small-molecule- and peptide-based inhibitors of the same protease—trypsin—to better understand how photoswitchable drugs interact with their biological target. The best peptidic inhibitor displayed a more than fivefold difference in inhibitory activity between isomeric states, whereas the best small-molecule inhibitor only showed a 3.4-fold difference. Docking and molecular modelling suggest this result is due to a large change in 3D structure in the key binding residues of the peptidic inhibitor upon isomerisation; this is not observed for the small-molecule inhibitor. Hence, we demonstrate that significant structural changes in critical binding motifs upon irradiation are essential for maximising the difference in biological activity between isomeric states. This is an important consideration in the design of future photoswitchable drugs for clinical applications.

Introduction

Off-target effects associated with a drug can be mitigated by controlling its activity in time and space.[1–4] This can be achieved photochemically using an approach referred to as photopharmacology.[2] Here a molecular photoswitch is incorporated into the structure of a drug, the geometry of which can be reversibly controlled on irradiation with light of a defined wavelength. The associated change in structure on irradiation with light must influence the molecule's interaction with its target, to modulate biological activity.[5,6] Such photoswitchable drugs have been reported to target ion channels,[7] receptors,[8] and enzymes,[9] for treatment of diseases such as cancers[10,11] and bacterial infections.[12]

Despite reports of numerous such photoswitchable drugs,[6,13] and also novel ways to deliver the required light source where and when required,[13,14] most reported examples only show a modest two- to tenfold difference in biological activity between isomers.[6] More recent studies have reported compounds with a $>$20-fold difference,[15] however still only a few reported photoswitchable drugs have been trialled in animal studies[13] and there are even fewer examples of human clinical trials.[16] It remains unclear how large the difference in activity needs to be between isomeric states at the cellular level to produce a significant and beneficial difference in physiological effect in humans. However, maximising this difference—with the "on" state showing strong potency and the "off" state showing minimal activity—remains of crucial importance to this field of research and future clinical applications of photoswitchable drugs.

A better fundamental understanding of how photoswitchable drugs interact with their biological target is needed to optimise this fold-difference. In this paper, we explore this concept with the design and testing of a series of small-molecule inhibitors and peptide-based inhibitors that target the same enzyme. Trypsin was selected for this study, as its structure is well-studied and characterised by crystallography.[17] It has a well-defined binding pocket,[18] and there are multiple potent small-molecule- and peptide-based inhibitors reported and characterised in the literature.[19–22] This enabled us to study the structural interaction between our inhibitors and the known 3D structure of trypsin, and also aided the design of compounds which feature modifications on reported inhibitors as discussed below. The inclusion of both small-molecule and peptidic inhibitors of the same protease allowed the effect of size, 3D structure, mechanism and binding interactions on photoswitchable inhibitory activity to be systematically investigated.

We chose spiropyran and azobenzene as photoswitches in this study (Figure 1). The spiropyran component of the

[a] K. A. Palasis, Dr. V. Peddie, D. J. L. Turner, Dr. X. Zhang, Dr. J. Yu, Prof. A. D. Abell
ARC Centre of Excellence for Nanoscale BioPhotonics (CNBP)
Institute for Photonics and Advanced Sensing (IPAS)
Department of Chemistry, The University of Adelaide
North Terrace, Adelaide SA 5005 (Australia)
E-mail: andrew.abell@adelaide.edu.au

[b] Dr. J. Yu
Guangxi Key Laboratory of Electrochemical and Magneto-chemical Functional Materials
College of Chemistry and Bioengineering
Guilin University of Technology
Guilin 541004 (P. R. China)

Supporting information for this article is available on the WWW under https://doi.org/10.1002/cbic.202300453

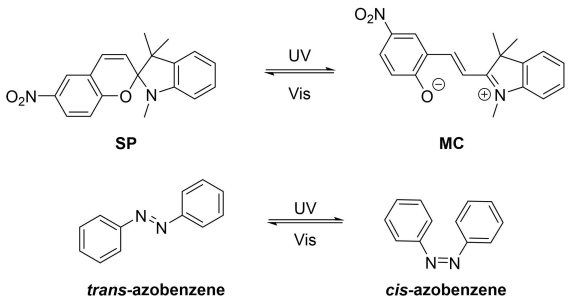

Figure 1. Photoisomerisation of spiropyran between the spiropyran (SP) and merocyanine (MC) states (top) and azobenzene between the *trans* and *cis* states (bottom).

small molecule inhibitors **1**, **2**, **5** and **6** incurs a large change in structure and polarity upon switching, from the uncharged spiropyran (SP) state to the zwitterionic merocyanine (MC) state after irradiation with UV light.[23] Azobenzene was chosen as the switch for the remaining small molecule inhibitors **3**, **4** and **7**, and the peptidic inhibitors **p1**–**p6**, as its switching between states is known to be particularly efficient and quantifiable,[24] whilst affecting a significant change in geometry and polarity suitable for influencing binding to trypsin.

The design of small molecules **1**–**7** and peptides **p1**–**p6** was based on well-studied and well-characterised inhibitors of trypsin reported in the literature.[19,20,25] These known inhibitors display potent anti-trypsin activities, have published co-crystal structures, and are also amenable to synthetic modification and therefore the inclusion of a photoswitchable group. The small-molecule series is described below, followed by the peptidic inhibitors.

Results and Discussion

Small molecules

The structures of the target inhibitors are shown in Figure 2. Compounds **1** and **3** are based on traditional small-molecule protease inhibitors,[26] with a methyl ester electrophile, an arginine residue at the pseudo P1 position, and the photoswitch bound via an amide bond.[26] Trypsin's S1 pocket contains a negatively charged aspartic acid residue (Asp189) and preferentially accommodates positively charged residues, specifically arginine.[18] Compounds **2** and **4** have the photoswitch bound via an amide linkage to a benzamidine unit. Benzamidine is well studied in the literature as a simple trypsin inhibitor, known to bind in the S1 pocket of trypsin with a K_i value of 19 μM.[19]

The inclusion of benzamidine was probed further in the design of **5** and **7**, where the benzamidine unit is incorporated directly onto the photoswitch, as part of the phenyl rings of the azobenzene or spiropyran moiety. It is noteworthy that the structure of **5** in its MC form very closely mimics the most potent reported trypsin inhibitor in the

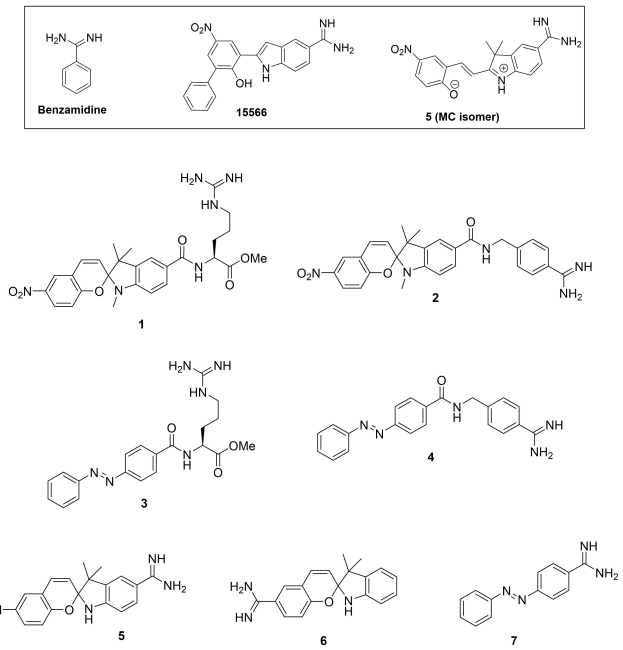

Figure 2. Structures of target small molecules **1**–**7**. Only one photochemical isomer, as defined in Figure 1, is shown. Inset: Structures of literature trypsin inhibitors benzamidine and **15566**[19,20] and MC isomer of **5.**

literature (**15566**, Figure 2)[20] which has a reported K_i value of 13 nM. Derivative **5** was therefore predicted to be the most active of the series, with the MC form of each spiropyran compound predicted to be the more potent isomer. Finally, **6** was designed to be structurally similar to **5**, but with the benzamidine unit instead incorporated onto the phenyl ring on the chromene side of spiropyran, to examine the effect of inserting the biologically active motif at the opposite end of the photoswitch. Both **5** and **6** lack a methyl substituent on the indoline nitrogen, a common feature in spiropyran-based photoswitchable molecules.[23] This deviation was made to better mimic the structure of **15566**, where crystal structures show the N–H on the indole of **15566** forms a hydrogen bond to Ser195 on trypsin which is important for binding.[20]

The syntheses of compounds **1**–**7** are outlined in Schemes 1, 2, 3 and 4 and described further in the Experimental Section. Compounds purified by RP-HPLC were isolated in diminished yield.

Compound **8** was formed by esterifying Boc-L-arginine hydrochloride hydrate with thionyl chloride in methanol. Spiropyran **10** was synthesised by reacting **9**[26] with 2-hydroxy-5-nitrobenzaldehyde and TEA in anhydrous ethanol at reflux. Spiropyran **10** was then coupled to **8**, using HCTU and DIPEA in DMF, to give **1** (13% yield). Derivative **10** was also coupled to 4-aminomethyl benzamidine dihydrochloride, using HATU and DIPEA in DMF, to give **2** (10%). Azobenzene **11** was prepared by reacting 4-aminobenzoic acid with nitrosobenzene in AcOH at 40 °C. The product of this reaction was then coupled to **8** (using the conditions described above for SP **1**) to give **3** (1%) and 4-aminomethyl benzamidine

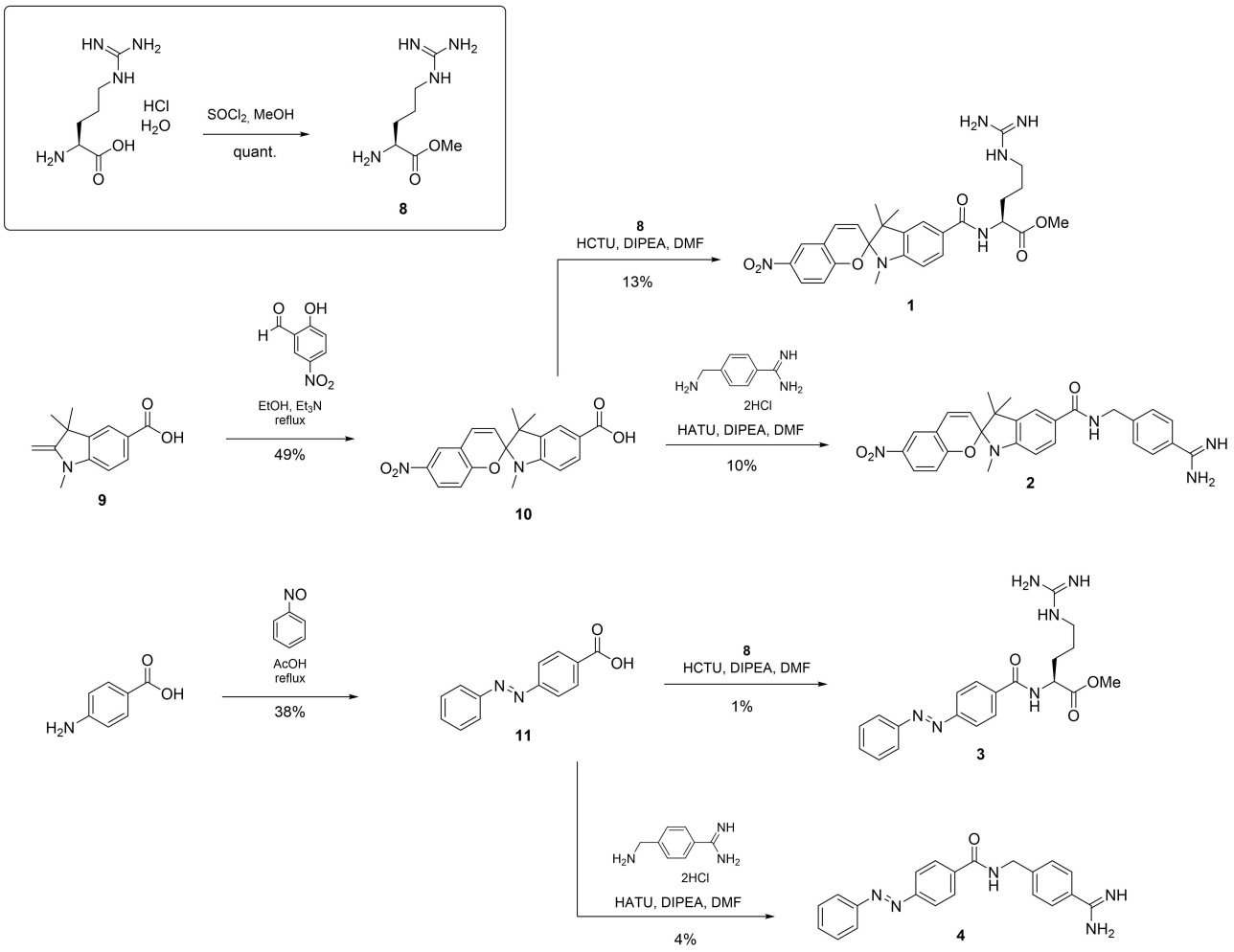

Scheme 1. Synthesis of **1**, **2**, **3** and **4**.

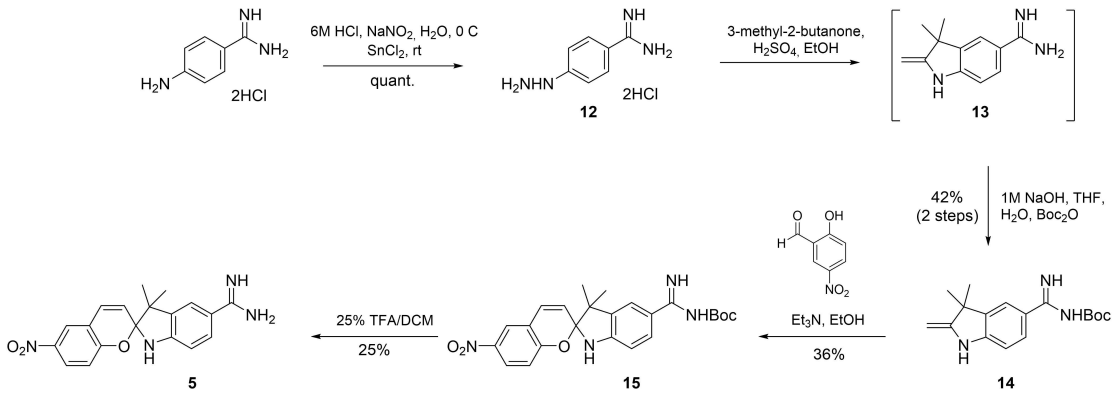

Scheme 2. Synthesis of **5.**

dihydrochloride (using the conditions described above for SP **2**) to form **4** (4%).

Following literature procedure,[27] a solution of 4-aminobenzamidine dihydrochloride in 6 M aqueous HCl was reacted with sodium nitrite in water, followed by tin(II) chloride, to give hydrazine **12**. Indoline **13** was formed on reaction of **12** with 3-methyl-2-butanone and sulphuric acid in ethanol. The amidine was Boc-protected, using 1 M aqueous NaOH, THF, H_2O and Boc_2O, to give **14**. SP **15** was then formed by reacting **14** with 2-hydroxy-5-nitrobenzaldehyde and TEA in anhydrous ethanol at reflux, in 36% yield. Multiple conditions were trialled to achieve successful Boc-deprotection of **15**, with 25% TFA in DCM for 10 min proving optimal. Purification of the crude material, by RP-HPLC, gave

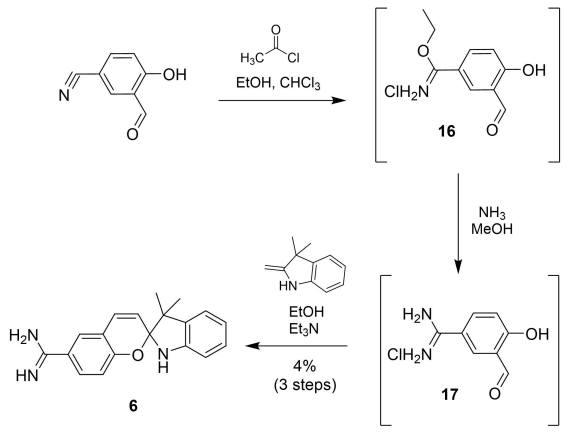

Scheme 3. Synthesis of **6**.

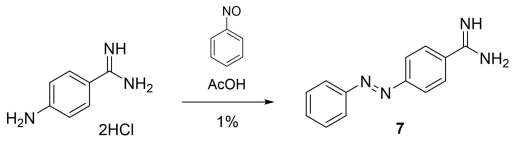

Scheme 4. Synthesis of **7**.

SP **5** in 25% yield. Imidate ester **16** was formed in a Pinner reaction;[28] 3-formyl-4-hydroxybenzonitrile in EtOAc was added to a solution of acetyl chloride in ethanol, at −78 °C, and the mixture left in the fridge for 5 days, to give **16**. This was then reacted with a solution of ammonia in methanol to give amidine **17**, which was subsequently treated with 2,3,3-trimethylindolenine and TEA in ethanol. The product SP **6** was isolated in 4% yield after purification by RP-HPLC. Azobenzene **7** was formed, in one step, by reacting 4-aminobenzamidine dihydrochloride with nitrosobenzene in AcOH at reflux (1%), as depicted in Scheme 4.

Compounds **1**–**7** were separately irradiated for 15 min (352 nm) in DMSO and Tris buffer, and the resulting photostationary states analysed by absorbance and fluorescence. NMR spectra were also collected in CD_3OD before and after irradiation for 1 h at 352 nm. Absorbance and fluorescence measurements provide qualitative information on switching, while integration of NMR signals was used to quantify the ratios of isomers. These data are presented in full in Figures S1–S4 in the Supporting Information, and are summarised in Table 1, for the thermally adapted state (TAS, before irradiation) and photostationary state (PSS, after irradiation).

NMR data—supported by absorbance and fluorescence data—show the TAS and PSS distributions of isomers varied greatly between compounds (Table 1). In particular, azobenzenes **3**, **4** and **7** switched more efficiently than spiropyrans **1**, **2**, **5** and **6**. Compound **4**, with its benzamidine group bound to the photoswitchable azobenzene unit via an amide bond, showed the greatest difference in isomeric composition between the two states with 89% *trans*-**4** in the TAS and 82% *cis*-**4** in the PSS.

Each separate isomeric state (TAS and PSS) of compounds **1**–**7** was assessed for anti-trypsin activity, using bovine trypsin and Boc-Phe-Ser-Arg-AMC as the fluorogenic substrate. IC_{50} values were calculated from a plot of measured initial reaction velocity relative to the positive control against the logarithm of inhibitor concentration (Figure S8). These IC_{50} values were then used to estimate K_i values of competitive inhibition,[29] as described in the Experimental Section and summarised in Table 2.

The TAS and PSS of compounds **1**–**7** all show reasonable inhibition of bovine trypsin, with low-/sub-micromolar activities. With the exception of **6** and **7**, each compound is more potent than the known inhibitor benzamidine ($K_i = 19$ μM) in both isomeric states.[19] Spiropyran **2** proved to be the most potent inhibitor of the series in both the TAS and PSS, however the observed activity difference between states is only 1.2-fold. This is likely due to modest switching of this

Table 2. K_i inhibition data for small molecules **1**–**7** against trypsin protease, in their respective states (TAS and PSS).

Cmpd	K_i [μM][a]		Fold-difference
	TAS non-irradiated	PSS irradiated	in activity
1	2.3 ± 0.1	2.1 ± 0.1	1.1
2	1.02 ± 0.06	0.82 ± 0.04	1.2
3	5.1 ± 0.1	2.4 ± 0.1	2.1
4	12.4 ± 0.7	3.6 ± 0.1	3.4
5	1.53 ± 0.05	2.1 ± 0.1	1.4
6	16.0 ± 0.5	35 ± 2	2.2
7	36 ± 2	80 ± 5	2.2

[a] Calculated from IC_{50} values (see the Experimental Section).

Table 1. TAS (non-irradiated) and PSS (irradiated: 15 min, 352 nm) distributions for SPs **1**, **2**, **5** and **6** and azobenzenes **3**, **4** and **7**. Ratios are calculated by integration of proton signals in NMR spectra.

Spiropyran compound	TAS non-irradiated (SP:MC)	PSS irradiated (SP:MC)	Azobenzene compound	TAS non-irradiated (*trans*/*cis*)	PSS irradiated (*trans*/*cis*)
1	100:0	N.D.[a]	3	91:9	27:73
2	100:0	N.D.[a]	4	89:11	18:82
5	49:51	70:30	7	87:13	28:72
6	45:55	86:14			

[a] No data for the irradiated PSS of **1** and **2** as the MC isomer is too unstable to be visualised by NMR spectroscopy.

compound upon irradiation, as revealed by the absorbance and fluorescence data (Figure S1). The PSS for both spiropyrans **5** and **6** show decreased activity compared to the respective TAS. These results are consistent with observations made from the earlier NMR spectra (Table 1), where the MC isomer decreases in concentration after UV irradiation. We expected the MC isomers to be more potent than the SP isomers for the spiropyran compounds; therefore, the TAS for spiropyrans **5** and **6** showed better anti-trypsin activity than the PSS due to a higher concentration of MC isomer. Azobenzene **4** showed the largest difference in activity between the two isomeric states (3.4-fold)—consistent with it showing the largest difference in TAS/PSS compositions—but weakened anti-trypsin activity compared to spiropyran **2**.

With the exception of **6**, spiropyrans **1**, **2**, and **5** all displayed improved anti-trypsin activity compared to the azobenzenes **3**, **4**, and **7**, likely due to structural similarity of the MC isomers with known trypsin inhibitor **15566**.[20] However, the azobenzene compounds provided a larger difference in activity between isomeric states—up to 3.4-fold, compared to maximum 2.2-fold for the spiropyran inhibitors. This is likely due to the larger differences in isomeric composition between the two states for the azobenzenes. Therefore, the azobenzene small molecules are better photoswitchable inhibitors of trypsin than the spiropyran small molecules.

Azobenzene **4**, with the largest difference in inhibitory activity between its two isomeric states (3.4-fold), was docked into the bovine trypsin active site to investigate the likely binding conformations of the TAS and PSS[30] (Figure 3). *Trans*-**4** was used to represent the *trans*-enriched TAS, and *cis*-**4** the *cis*-enriched PSS. ICM software was used to dock both isomers of **4** onto bovine trypsin, co-crystallised with benzamidine (PDB ID: 3ATL[30]). 3ATL shows benzamidine binds in the S1 pocket of trypsin, with hydrogen bonds between the amidine group and Asp189 as expected.[18,30]

Figure 3 shows the benzamidine motif of **4** also binds into the S1 pocket (close to Asp189), however the azobenzene moiety does not appear to fit inside this pocket and is as such aligned outside it. Hence, the azobenzene group is unlikely to significantly impact the binding affinity, which is known to depend heavily on interactions inside the S1 pocket.[18] The benzamidine motif, which is bound inside this pocket, is thus likely to be the main contributor toward the activity of the inhibitor. The positioning of the benzamidine group inside the S1 pocket is very similar in both *trans*- and *cis*-**4**.

Therefore, we postulate that the observed modest 3.4-fold difference in affinity between the two isomeric states of **4** is likely due to the switchable azobenzene moiety neither being directly involved in binding, nor changing the confirmation of the benzamidine group which is responsible for the anti-trypsin activity. To manifest a larger difference in biological activity between isomeric states, significant structural changes upon irradiation are required in the moieties essential to binding. As such, we believed that a small-molecule-based approach to inhibitors (as in **1**–**7**) would not exploit the small size of the active site (S1 pocket) in trypsin.[30]

We thus considered an alternative approach to photoswitchable inhibitors in order to optimise photoswitching and differences in activity. Peptidic-based inhibitors were next investigated as described in the following section.

Peptides

Peptides **p1**–**p6** (Figure 4) were designed based on inhibitor **p-SFTI**[25] (Figure 4, inset), a reported cyclic peptidic trypsin inhibitor, that itself is based off sunflower trypsin inhibitor 1.[25] Analogues of **p-SFTI1** containing a photoswitchable diarylethene moiety have recently been reported with effective modulation of biological activity between isomers,[31] demonstrating the suitability of this peptide for photoswitchable studies. **p-SFTI** has a reported K_i value of 103 nM—its activity is due to its rigid secondary structure, due to a well-defined β-hairpin loop.[25] Literature suggests that a *cis*-azobenzene mimics a β-turn in peptides.[32] Therefore, we postulated that replacing the L-Pro5-D-Pro6 β-turn motif of peptide **p-SFTI** with an azobenzene unit could enable photocontrol of trypsin activity. The *cis* isomer of the photoswitch should position the peptide into the active, β-hairpin structure, while the *trans* isomer should position the

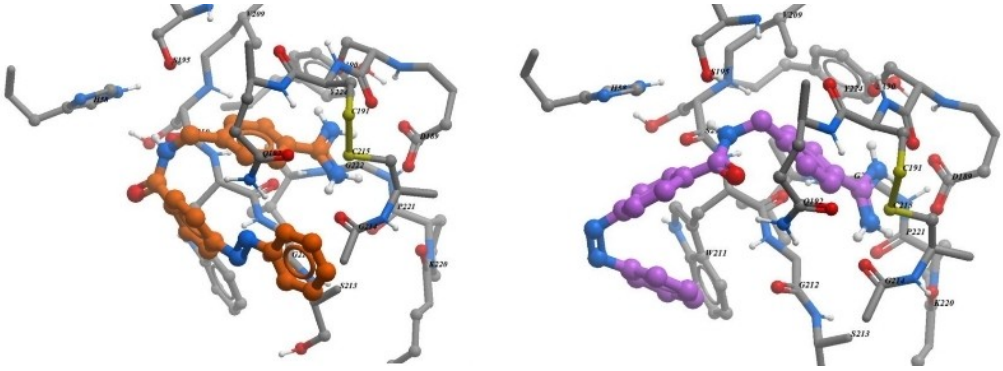

Figure 3. Docked conformations of *trans*-**4** (left, orange) and *cis*-**4** (right, purple) in bovine trypsin (PBD ID: 3ATL[30]).

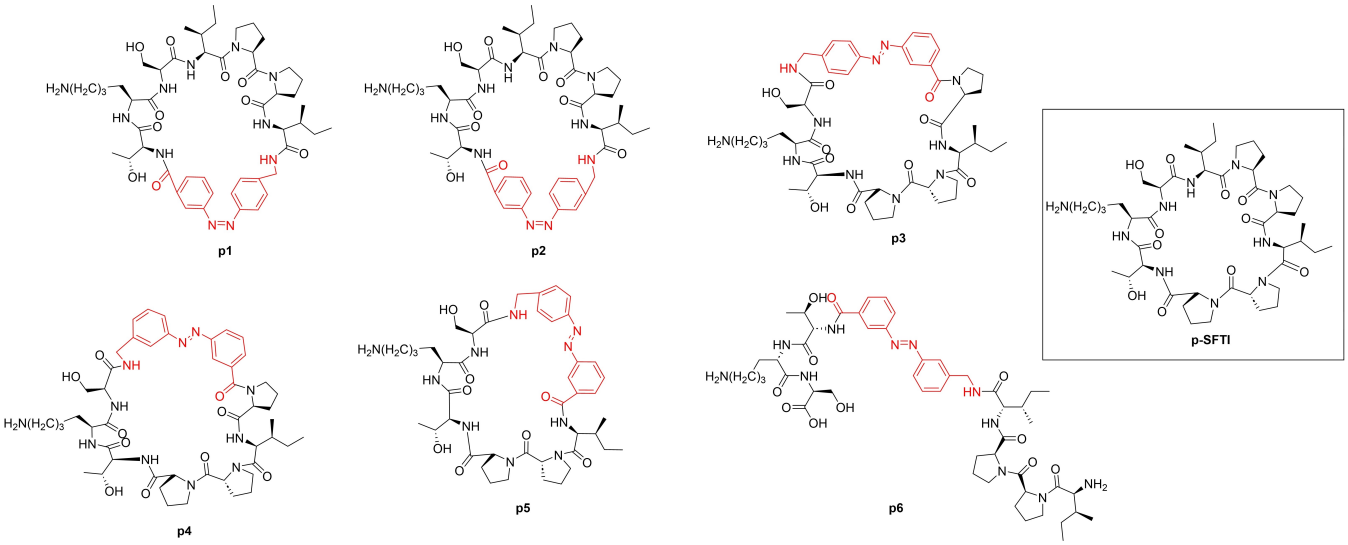

Figure 4. Structures of target peptides **p1**–**p6**, with azobenzene groups highlighted in red. Inset: Structure of peptide **p-STFI**.[25]

peptide into an unfolded structure that doesn't bind as well to trypsin.

The target peptides **p1**–**p6** have the key azobenzene unit incorporated into the peptide backbone, at different locations around the ring. Peptides **p1** and **p2** have the azobenzene in place of the L-Pro5-D-Pro6 resides of **p-STFI**, peptides **p3** and **p4** have the azobenzene replacing the Ile4-Pro5 residues, and **p5** has the azobenzene replacing the Ile4-D-Pro6 residues. The azobenzene linkages to the rest of the macrocycle were also varied to determine the effect on activity and switching; peptides **p1**, **p3** and **p5** all have *para*, *meta* linkages to the rest of the macrocycle, while **p2** and **p4** have *meta*, *meta* linkages. Finally, the linear peptide **p6** was designed to validate the importance of the macrocycle for activity—this peptide represents the linear version of macrocycle **p2**.

Peptides **p1**–**p6** (Figure 4) were prepared by solid phase peptide synthesis (SPPS) on 2-chlorotrityl functionalised polystyrene resin, as described in the Experimental Section. Scheme 5 summarises the synthesis of peptide **p2** as a representative example, with peptides **p1**–**p6** presenting different amino acid sequences and/or azobenzene substitutions (*meta*, *meta* or *para*, *meta*). The component azobenzene units of **p1**–**p6** were prepared and incorporated into the peptide sequence as described in literature.[33] SPPS gave the linear sequences of each peptide, which were subsequently cleaved from the resin. Linear peptides **p1**–**p5** were irradiated at 352 nm for 18 h to give the corresponding *cis* isomers, which brings the termini closer to facilitate cyclisation on subsequent treatment with HATU. Cyclisation was performed overnight under further UV irradiation. The component *t*Bu and Boc protecting groups were removed on treatment with TFA in DCM to give the desired cyclic peptides **p1**–**p5**, which were purified by RP-HPLC. Peptide **p6** was purified by RP-HPLC in its linear form.

Solutions of peptides **p1**–**p6** were then separately irradiated for 15 min at 352 nm, and analysed using the methodology described above for the small molecules. Each peptide was switched in DMSO and Tris buffer for analysis by absorbance spectroscopy, and in CD_3OD for NMR analysis. These data are summarised in Table 3, with full data presented in Figures S5–S7.

The absorbance data show efficient switching from the *trans* to *cis* isomer upon UV irradiation for each peptide **p1**–**p6**, which is consistent in the NMR data. In all peptides, there is $\geq$74% *trans* isomer in the TAS, and the azobenzene switches efficiently to $\geq$85% *cis* isomer in the PSS. Of all the peptides, **p6** gave the highest % *trans* in the TAS and PSS, which indicates that the linear structure of **p6** favours a *trans* conformation more so than the cyclic structures of **p1**–**p5**. There is no clear trend in the effect of a *para*, *meta* substitution (of peptides **p1**, **p3** and **p5**) compared to a *meta*, *meta* substitution (**p2** and **p4**) on the PSS or TAS isomeric distributions.

Peptides **p1**–**p6** were next assayed against bovine trypsin, as described earlier for the small molecules. The K_i values were calculated for all peptides in both isomeric states, as

Table 3. TAS (non-irradiated) and PSS (irradiated: 1 h, 352 nm) distributions for peptides **p1**–**p6**. Ratios are calculated by integration of proton signals in NMR spectra.

Peptide	TAS non-irradiated (*trans*:*cis*)	PSS irradiated (*trans*:*cis*)
p1	83:17	11:89
p2	74:26	10:90
p3	71:29	5:95
p4	78:22	9:91
p5	75:25	7:93
p6	92:8	15:85

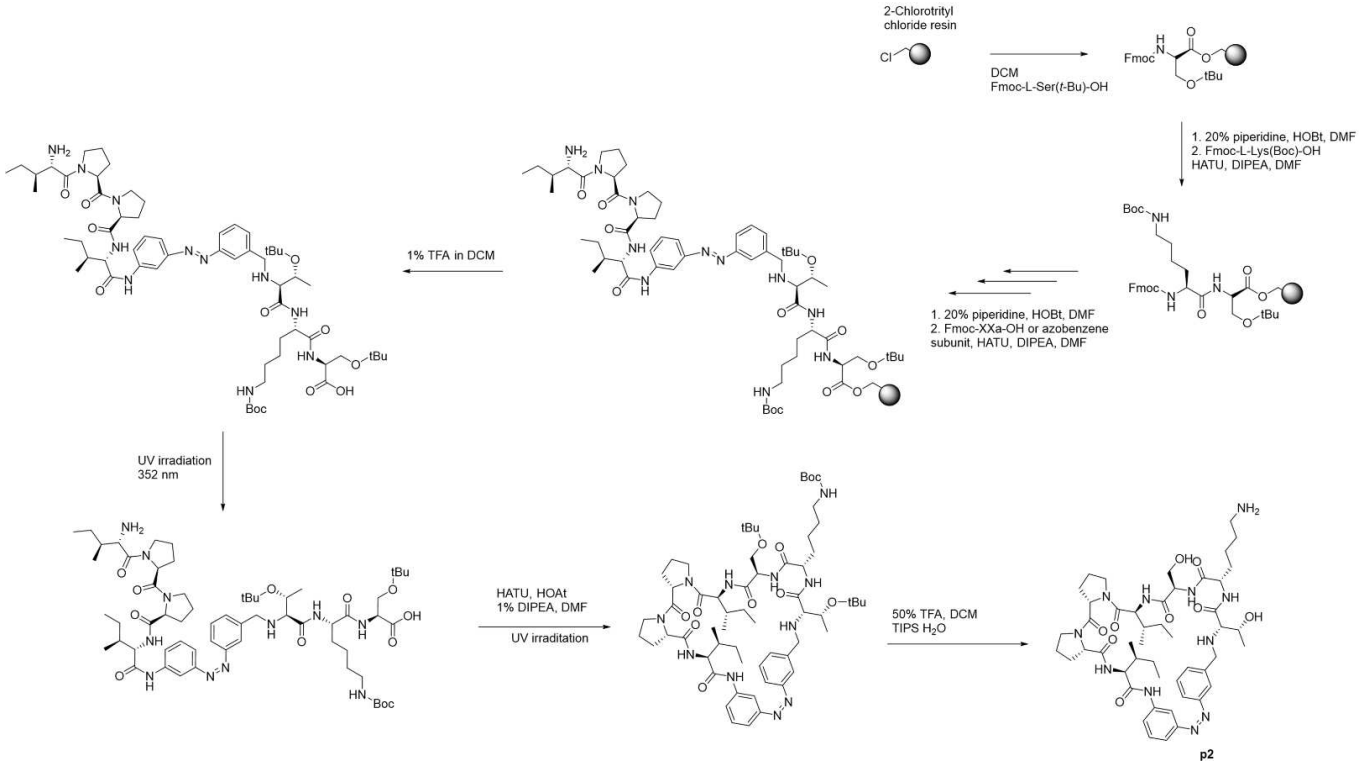

Scheme 5. Synthesis of peptide **p2**. The linear peptide was synthesised by SPPS, and subsequently cleaved from the resin, cyclised, deprotected and purified by RP-HPLC.

summarised in Table 4. Plots of log[I] against *v* [%] are displayed in Figure S9.

Across all peptides, there is no clear trend in potency of inhibitors or fold-difference between states based on *meta*, *meta* or *meta*, *para* substitution of the azobenzene. Peptide **p5** lacked anti-trypsin activity, suggesting inclusion of the azobenzene at the Ile4-D-Pro6 position on the macrocycle is detrimental to inhibition. Linear peptide **p6** also lacked activity against trypsin, compared to its cyclic and particularly potent analogue **p2**. This is consistent with the known importance of the macrocycle in peptidic inhibitors of trypsin.[25] Peptide **p2** was the most active inhibitor of the series with a $K_i = 7.4\ \mu M/2.56\ \mu M$ in the TAS/PSS; however, **p3** showed the largest fold-difference between states (> 5 times). This large activity difference, due to potency of 16.1 μM in the PSS compared to no activity (> 86 μM) in the TAS, indicates that peptide **p3** is the best photoswitchable inhibitor from this peptide series.

Table 4. K_i inhibition data for peptides **p1**–**p6** against trypsin protease, in their respective states (TAS and PSS).

Peptide	K_i [μM][a]		Fold difference
	TAS non-irradiated	PSS irradiated	in activity
p1	71 ± 3	30 ± 1	2.3
p2	7.4 ± 0.2	2.56 ± 0.06	2.9
p3	> 86	16.1 ± 0.4	> 5
p4	32 ± 2	17.6 ± 0.5	1.8
p5	> 86	> 86	–
p6	> 86	> 86	–

[a] Calculated from IC_{50} values (see the Experimental Section)-

The more than fivefold activity difference observed for peptide **p3** is larger than the 3.4-fold difference for the optimal small molecule **4** described above. This suggests that any structural change resulting from irradiation of peptide **p3** has more of an effect on the binding affinity to trypsin compared with the small molecules.

Peptides **p2** and **p3** were modelled in the lowest-energy conformations using the NWChem 6.6 package—described further in the Experimental Section—for both *trans* and *cis* isomers (representing the TAS and PSS, respectively; Figure 5). These were then compared to the lowest-energy conformation of the known inhibitor **p-SFTI** (Figure 5) to better understand the trends in K_i data. In **p-SFTI**, the β-turn is induced by the L-Pro-D-Pro residues,[25] and is observed on the right-hand side of the structure in Figure 5. A *cis*-azobenzene moiety in *cis*-**p2** mimics the β-turn in **p-SFTI** and aligns the other residues of *cis*-**p2** very similarly to **p-SFTI**. This supports the experimental K_i data which shows that **p2** is the most potent peptidic inhibitor of the series. In contrast, the *trans*-azobenzene group in *trans*-**p2** does not appear to mimic a β-turn with the overall macrocyclic structure differing significantly from **p-SFTI**, resulting in reduced activity compared to *cis*-**p2**.

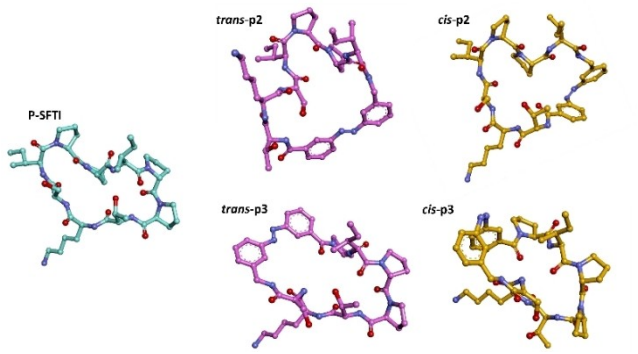

Figure 5. Lowest-energy conformations of **p-STFI**[25] (grey), *trans*-**p2** (purple), *cis*-**p2** (orange), *trans*-**p3** (purple) and *cis*-**p3** (orange). Conformations were modelled by using NWChem 6.6.[34]

Interestingly, despite these structural differences, the fold-difference in activity between the TAS/PSS of **p2** is not as large as that observed for peptide **p3**. In **p3**, the β-turn (induced by the L-Pro-D-Pro residues[25]) is retained in both isomers; the azobenzene was placed on the opposite side of the macrocycle to the β-turn to determine its effect at this position. As can be seen in Figure 5, the overall 3D structures of *trans*- and *cis*-**p3** are very different to one another. Notably, the location of residues Thr1 and Pro6, and the overall rigidity of the macrocycle, varies greatly between the two isomers. This results in a fivefold difference in biological activity, suggesting that for peptides **p1**–**p6**, not only is a β-turn important for binding to trypsin but so is the orientation of other residues and the overall rigidity of the macrocycle.

The modelling and K_i data discussed above suggest that, at least for trypsin, macrocyclic peptides make better photoswitchable inhibitors than small molecules, as they can induce a larger difference in biological activity between isomeric states. The inhibitory activity of peptides **p1**–**p6** is defined by the overall shape of the macrocycle and alignment of multiple residues, compared to inhibition by benzamidine-based small molecules **1**–**7**, which depends solely on interactions inside the P1 pocket. *Trans*/*cis* isomerisation in the peptides, as in **p3**, therefore causes a larger fold-difference in activity, due to more significant effects on 3D structure.

Conclusions

In this work, a series of small-molecule photoswitchable inhibitors (**1**-**7**) and a series of cyclic peptidic photoswitchable inhibitors (**p1**–**p6**) of the protease trypsin were designed, synthesised and assayed in two isomeric states, the TAS (before irradiation) and PSS (after irradiation). Spiropyran **2** was found to be the most potent small-molecule inhibitor, with a K_i of 1.02 μM in the TAS and 0.82 μM in the PSS, while azobenzene **4** had the largest difference (3.4-fold) in anti-trypsin activity between isomeric states for small molecules **1**–**7**. However, in-silico docking of **4** with trypsin showed the azobenzene unit was unlikely to be directly involved in binding in the S1 pocket, and hence the small-molecule approach to trypsin inhibitors is unlikely to result in an optimum photoswitchable inhibitor. Peptide **p2** showed the most potent activity of the peptide-based inhibitors, with $K_i = 7.4$ μM in the TAS and 2.56 μM in the PSS; however, **p3** showed the largest fold-difference between isomeric states (> 5 times). Lowest-energy-confirmation modelling suggests that isomerisation between *trans*-**p3** and *cis*-**p3** induces a very large change in the overall 3D structure of peptide **p3**. Therefore, the cyclic-peptide approach is more favourable for photoswitchable inhibitors of trypsin, as the large structural change in the macrocycle upon irradiation results in a greater difference in biological activity between isomeric states.

This work demonstrates that many structural factors—such as the positioning of key binding residues and overall structural rigidity—must be considered when designing a photoswitchable inhibitor in order to optimise the difference in biological activity between isomeric states. This can be achieved by designing the inhibitor to significantly change 3D structure upon irradiation in a way that affects binding (e.g., in a macrocyclic peptide); or by incorporating the most important functional group for binding close to the switch, so that it changes conformation significantly upon isomerisation. Maximising the fold-difference in activity ensures the photoswitchable inhibitor acts as a viable "switch", thereby helping to bring these drugs closer to a future clinical application.

Experimental Section

Unless otherwise stated, all starting materials, enzymes, reagents and solvents were purchased from Merck (NSW, Australia) and were used without further purification. All amino acids, coupling reagents and resins were purchased from Chem-Impex International, Inc (IL, USA). All amino-acids are L-configuration unless otherwise specified. ^{1}H and ^{13}C NMR spectra were recorded on a Varian 500 MHz/Varian Inova 600 MHz instrument in the indicated solvents. Chemical shifts are reported in ppm (δ). High resolution mass spectra were recorded on an Agilent 6230 TOF LC/MS fitted with an Agilent 1260 Infinity HPLC unit. Where indicated, compounds were analysed and purified by reversed-phase (RP-) HPLC, using an Agilent 1260 Infinity LC system equipped with a Phenomenex Luna C-18(2) column (250×4.6 mm) for analytical traces; and a Gilson GX-Prep HPLC system equipped with a Phenomenex Luna C-18(2) column (250×10 mm) or a Phenomenex Phenyl-Hexyl column (250×10 mm) for semi-preparative purification. H_2O/TFA (100 : 0.1 *v/v*) and MeCN/TFA (100 : 0.1 *v/v*) were used as aqueous and organic buffers. All graphs were generated using GraphPad Prism 9 software. A Sankyo Penki F8T5 352 nm 8 W bulb was used for photoswitching experiments. A Synergy H4 Hybrid Multi-Mode Microplate Reader was used with black walled, clear bottomed 96 well plates (Corning, Australia) for photoswitching experiments and trypsin assays.

(*S*)-Methyl 2-amino-5-guanidinopentanoate (8): To a stirring solution of Boc-L-arginine hydrochloride hydrate (250 mg, 0.76 mmol) in anhydrous methanol (2.5 mL) in an ice-water bath was added thionyl chloride (0.11 mL, 1.52 mmol) dropwise. The reaction mixture was stirred at RT under N_2 for 18 h. The excess

methanol and thionyl chloride were removed under reduced pressure to afford **8** as a white foam (214 mg, quant.). ^{1}H NMR (500 MHz, CD_3OD): $\delta = 4.11$ (t, $J = 6.5$ Hz, 1H), 3.86 (s, 3H), 3.26 (t, $J = 7.0$ Hz, 2H), 2.08-1.90 (m, 2H), 1.85-1.64 (m, 2H).

1′,3′,3′-Trimethyl-6-nitrospiro[chromene-2,2′-indoline]-5′-carboxylic acid (10): To a suspension of **9** (500 mg, 2.30 mmol) and 2-hydroxy-5-nitrobenzaldehyde (385 mg, 2.30 mmol) in anhydrous ethanol (5 mL) was added triethylamine (1.21 mL, 2.30 mmol). The reaction mixture was heated at reflux under N_2 for 24 h. The ethanol was removed under reduced pressure and the crude product purified by flash column chromatography on silica (1-10% MeOH/DCM) to afford **10** as an orange solid (414 mg, 49%). ^{1}H NMR (500 MHz, [D_6]DMSO): $\delta = 12.09$ (s, 1H), 7.98 (d, $J = 2.8$ Hz, 1H), 7.76 (dd, $J = 9.0$, 2.8 Hz, 1H), 7.55 (dd, $J = 8.2$, 1.5 Hz, 1H), 7.41 (d, $J = 1.2$ Hz, 1H), 7.00 (d, $J = 10.4$ Hz, 1H), 6.66 (d, $J = 9.0$ Hz, 1H), 6.43 (d, $J = 8.2$ Hz, 1H), 5.76 (d, $J = 10.4$ Hz, 1H), 2.50 (s, 3H), 0.98 (s, 3H), 0.87 (s, 3H).

4-(Phenyldiazenyl)benzoic acid (11): Nitrosobenzene (250 mg, 2.33 mmol) and 4-aminobenzoic acid (352 mg, 2.57 mmol) were dissolved in acetic acid (5 mL, and the solution was stirred at 40 °C for 48 h. The resulting precipitate was collected by vacuum filtration to afford **11** as an orange solid (200 mg, 38%). ^{1}H NMR (500 MHz, [D_6]DMSO): $\delta = 13.21$ (s, 1H), 8.18–8.12 (m, 2H), 8.00–7.91 (m, 4H), 7.67–7.58 (m, 3H).

(2*S*)-Methyl 5-guanidino-2-(1′,3′,3′-trimethyl-6-nitrospiro[chromene-2,2′-indolin]-5′-ylcarboxamido)pentanoate (1): To a suspension of 8 (67 mg, 0.57 mmol) and 10 (208 mg, 0.57 mmol) in anhydrous DMF (3 mL) was added HCTU (281 mg, 0.68 mmol). DIPEA (0.39 mL, 2.27 mmol) was added dropwise to the reaction mixture, which was stirred at RT under N_2 for 24 h. Water (20 mL) was added to the reaction mixture, which was then extracted with EtOAc (×3). The combined extracts were washed with $NaHCO_3$ followed by water and brine, and then dried over Na_2SO_4, filtered, and concentrated under reduced pressure. The crude product was purified by flash column chromatography on silica (2–15% MeOH/DCM + 1% TFA) to afford **1** as a pink solid (30 mg, 13%). ^{1}H NMR (599 MHz, CD_3OD): $\delta = 8.13$ (d, $J = 2.7$ Hz, 1H), 8.05 (dd, $J = 9.0$, 2.8 Hz, 1H), 7.79 (dd, $J = 8.2$, 1.8 Hz, 1H), 7.66 (d, $J = 1.8$ Hz, 1H), 7.14 (d, $J = 10.4$ Hz, 1H), 6.81 (d, $J = 8.9$ Hz, 1H), 6.65 (d, $J = 8.2$ Hz, 1H), 6.00 (d, $J = 10.3$ Hz, 1H), 4.68 (dd, $J = 9.6$, 5.1 Hz, 1H), 3.76 (d, $J = 1.4$ Hz, 3H), 3.30–3.20 (m, 3H), 2.82 (s, 3H), 2.05 (dddd, $J = 14.2$, 9.4, 6.7, 5.2 Hz, 1H), 1.89 (dtd, $J = 14.4$, 9.5, 5.2 Hz, 1H), 1.80-1.65 (m, 2H), 1.34 (s, 3H), 1.22 (s, 3H); ^{13}C NMR (151 MHz, CD_3OD): $\delta = 174.12$, 170.42, 160.63, 158.64, 152.57, 142.72, 137.86, 129.93, 129.83, 126.81, 125.73, 123.89, 122.21, 122.11, 120.36, 116.43, 107.70, 107.34, 53.56, 53.15, 52.86, 41.90, 29.63, 28.98, 26.52, 26.16, 20.12; HRMS ESI+ (*m/z*) calcd for $C_{27}H_{32}N_6O_6$: 537.2456 $[M+H]^+$, found: 537.2452.

(*S*)-Methyl 5-guanidino-2-(4-(phenyldiazenyl)benzamido)pentanoate (3): To a solution of **11** (90 mg, 0.40 mmol) and **8** (47 mg, 0.40 mmol) in anhydrous DMF (2 mL) was added HCTU (197 mg, 0.48 mmol). DIPEA (0.28 mL, 1.59 mmol) was added dropwise to the reaction mixture, which was stirred at RT, under N_2, for 1 h. Water (20 mL) was added to the reaction mixture, which was extracted with EtOAc (×3). The extracts were washed with $NaHCO_3$ followed by water and brine, and then dried over Na_2SO_4, filtered, and concentrated under reduced pressure. The crude product was purified by RP-HPLC (20-100% MeCN/H_2O) to afford **3** as an orange solid (2 mg, 1%) (5:1 mixture of *E:Z* isomers). ^{1}H NMR (599 MHz, CD_3OD) *E* isomer from mixture: $\delta = 8.07$–8.02 (m, 2H), 8.02-7.98 (m, 2H), 7.97–7.94 (m, 2H), 7.61–7.52 (m, 3H), 4.71 (dd, $J = 9.5$, 5.1 Hz, 1H), 3.78 (s, 3H), 3.26 (td, $J = 7.6$, 6.5 Hz, 2H), 1.95–1.62 (m, 3H); *Z* isomer from mixture: $\delta = 7.80$–7.75 (m, 2H), 7.32–7.25 (m, 2H), 7.21–7.16 (m, 1H), 6.95–6.90 (m, 2H), 6.89–6.84 (m, 2H), 4.62 (dd, $J = 9.5$, 5.1 Hz, 1H), 3.74 (s, 3H), 3.25-3.19 (m, 2H), 2.12-2.03 (m, 3H); ^{13}C NMR (151 MHz, CD_3OD) mixture of *E* and *Z* isomers: δ 173.73, 169.64, 169.33, 158.67, 157.89, 155.85, 154.88, 153.96, 137.02, 133.53, 132.97, 130.40, 129.98, 129.72, 129.42, 128.98, 124.06, 123.77, 121.64, 121.24, 53.83, 53.74, 52.93, 52.89, 41.88, 29.52, 29.43, 26.54, 26.47; HRMS ESI+ (*m/z*) calcd for $C_{20}H_{24}N_6O_3$: 397.1983 $[M+H]^+$, found: 397.1993.

***N*-(4-Carbamimidoylbenzyl)-1′,3′,3′-trimethyl-6-nitrospiro[chromene-2,2′-indoline]-5′-carboxamide (2)**: To a solution of **10** (100 mg, 0.27 mmol) in anhydrous DMF (3 mL) was added HATU (103 mg, 0.27 mmol) and 4-aminomethyl benzamidine dihydrochloride (73 mg, 0.33 mmol). The mixture was stirred in an ice-water bath under N_2 for 15 min. DIPEA (0.19 mL, 1.09 mmol) was added dropwise to the reaction mixture, which was stirred at RT for 18 h. 1 M HCl (5 mL) was added to the reaction mixture, which was extracted with EtOAc (×3). The combined organic extracts were washed with water, followed by 1 M HCl, then $NaHCO_3$ and brine. The organic layer was dried over Na_2SO_4, filtered, and concentrated under reduced pressure. The crude product was purified by flash column chromatography on silica (0–20% MeOH/DCM) to afford **2** as a red solid (13 mg, 10%). ^{1}H NMR (500 MHz, [D_6]DMSO) $\delta = 9.25$ (s, 2H), 8.90 (t, $J = 6.0$ Hz, 1H), 8.81 (s, 2H), 8.24 (d, $J = 2.8$ Hz, 1H), 8.02 (dd, $J = 9.0$, 2.8 Hz, 1H), 7.81-7.74 (m, 3H), 7.69 (d, $J = 1.8$ Hz, 1H), 7.53 (d, $J = 8.2$ Hz, 2H), 7.25 (d, $J = 10.4$ Hz, 1H), 6.89 (d, $J = 9.0$ Hz, 1H), 6.70 (d, $J = 8.2$ Hz, 1H), 6.02 (d, $J = 10.4$ Hz, 1H), 4.55 (d, $J = 5.9$ Hz, 2H), 2.75 (s, 3H), 1.25 (s, 3H), 1.14 (s, 3H); ^{13}C NMR (126 MHz, [D_6]DMSO): $\delta = 166.40$, 165.38, 159.09, 150.10, 146.65, 140.74, 135.83, 128.52, 128.22, 128.17, 127.55, 126.40, 125.84, 125.24, 122.91, 121.03, 120.99, 118.88, 115.43, 106.22, 106.07, 51.70, 42.39, 28.48, 25.62, 19.64; HRMS (*m/z*) calcd for C28H27N5O4: 498.2136 $[M+H]+$, found: 498.2136.

***N*-(4-Carbamimidoylbenzyl)-4-(phenyldiazenyl)benzamide (4)**: To a suspension of **11** (60 mg, 0.27 mmol) and 4-aminomethyl benzamidine·2HCl (118 mg, 0.53 mmol) in anhydrous DMF (20 mL) was added HCTU (263 mg, 0.64 mmol). DIPEA (0.37 mL, 2.12 mmol) was added dropwise to the reaction mixture, which was stirred at RT under N_2 for 30 min. Water (50 mL) was added to the reaction mixture, which was basified to pH 14 using 4 M NaOH. The mixture was extracted with EtOAc (×3) and the extracts washed with $NaHCO_3$ followed by water and brine. The extracts were then dried over Na_2SO_4, filtered, and concentrated under reduced pressure. The crude product was purified by RP-HPLC (20–100% MeCN/H_2O) to afford **4** as a yellow solid (4 mg, 4%; 4:1 ratio of *E:Z* isomers). ^{1}H NMR (500 MHz, [D_6]DMSO) *E* isomer from mixture: $\delta = 9.37$ (t, $J = 5.9$ Hz, 1H), 9.26 (s, 2H), 8.94 (s, 2H), 8.14–8.08 (m, 2H), 8.01-7.96 (m, 2H), 7.94 (dd, $J = 7.8$, 1.9 Hz, 2H), 7.80–7.76 (m, 2H), 7.67–7.60 (m, 3H), 7.57 (d, $J = 8.2$ Hz, 2H), 4.60 (d, $J = 5.9$ Hz, 2H); ^{1}H NMR (500 MHz, [D_6]DMSO) *Z* isomer from mixture: $\delta = 9.16$ (t, $J = 5.9$ Hz, 1H), 9.26 (s, 2H), 8.94 (s, 2H), 8.14–8.08 (m, 2H), 7.80-7.76 (m, 2H), 7.76-7.73 (m, 2H), 7.51 (d, $J = 8.1$ Hz, 2H), 7.31 (t, $J = 7.9$ Hz, 2H), 7.18 (t, $J = 7.4$ Hz, 1H), 6.97–6.92 (m, 2H), 6.90–6.84 (m, 2H), 4.51 (d, $J = 6.0$ Hz, 2H); ^{13}C NMR (151 MHz, CD_3OD) mixture of *E* and *Z* isomers: $\delta = 169.42$, 168.31, 155.82, 153.97, 147.32, 137.26, 132.97, 130.40, 129.98, 129.54, 129.30, 129.23, 129.18, 128.31, 124.06, 123.85, 121.64, 121.33, 44.23; HRMS ESI+ (*m/z*) calcd for $C_{21}H_{19}N_5O$: 358.1662 $[M+H]^+$, found: 358.1664.

4-(Phenyldiazenyl)benzimidamide (7): 4-Aminobenzamidine·2HCl (100 mg, 0.48 mmol) and nitrosobenzene (77 mg, 0.72 mmol) were suspended in AcOH (5 mL) and the mixture heated at reflux for 24 h. The mixture was diluted with water (10 mL), basified to pH 14 with 4 M NaOH and extracted with

EtOAc (×3). The aqueous layer was filtered to remove the solid residue and then re-extracted with EtOAc (×2). The organic extracts were combined and washed with $NaHCO_3$ followed by water and brine, then dried over $MgSO_4$, filtered, and concentrated under reduced pressure. The crude product was purified by RP-HPLC (20-100% MeCN/H2O) to afford **7** as a pink solid (1 mg, 1%; 6:1 ratio of *E:Z* isomers). ^{1}H NMR (599 MHz, CD_3OD) *E* isomer from mixture: δ = 8.13–8.08 (m, 2H), 8.02–7.95 (m, 4H), 7.63–7.56 (m, 3H); ^{1}H NMR (599 MHz, CD_3OD) *Z* isomer from mixture: δ = 7.75–7.70 (m, 2H), 7.31–7.25 (m, 2H), 7.23–7.16 (m, 1H), 7.08-7.03 (m, 2H), 6.91–6.86 (m, 2H); ^{13}C NMR (151 MHz, CD_3OD) mixture of *E* and *Z* isomers: δ = 168.02, 157.08, 153.88, 133.49, 131.47, 130.50, 130.37, 124.32, 124.27; HRMS ESI+ (*m/z*) calcd for $C_{13}H_{12}N_4$: 225.1135 $[M+H]^+$, found: 225.1137.

4-Hydrazinylbenzimidamide dihydrochloride (12): 4-Aminobenzamidine dihydrochloride (200 mg, 0.96 mmol) was suspended in 6 M HCl (3 mL) and the mixture cooled in an ice-water bath. A solution of sodium nitrite (73 mg, 1.06 mmol) in water (1 mL) was added dropwise to the reaction mixture with vigorous stirring. The mixture was stirred in the ice-water bath for a further 30 min. Tin(II) chloride (395 mg, 1.92 mmol) was added in portions to the reaction mixture, which was stirred for 20 min and allowed to warm to RT. The solvent was removed under reduced pressure and the residue triturated with ethanol. The solid was collected by suction filtration and washed with absolute ethanol to afford **12** as an off-white solid (215 mg, quant.). ^{1}H NMR (500 MHz, [D_6]DMSO): δ = 10.21 (s, 3H), 9.11 (s, 2H), 9.00 (s, 1H), 8.80 (s, 2H), 7.76 (d, *J* = 8.8 Hz, 2H), 7.02 (d, *J* = 8.8 Hz, 2H).

***tert*-Butyl ((3,3-dimethyl-2-methyleneindolin-5-yl)(imino)methyl)carbamate (14)**: To a suspension of **12** (215 mg, 0.96 mmol) in 3-methylbutan-2-one (91 mg, 1.06 mmol) and anhydrous ethanol (15 mL) under N_2 was added conc. sulphuric acid (2 drops). The mixture was heated at reflux under N_2 overnight. Water (50 mL) was added and the mixture was washed with DCM (2×50 mL). The aqueous layer was basified to pH 14 with 4 M aqueous NaOH and extracted with DCM (4×50 mL). The combined organic extracts were dried over $MgSO_4$, filtered and concentrated under reduced pressure to afford crude **13** as a red/brown oil (153 mg) which was used in the following reaction without further purification.

To a mixture of **13** (126 mg,0.63 mmol) and 1 M NaOH (2 mL) in 50:50 THF/H_2O (1 mL) was added Boc anhydride (150 mg, 0.69 mmol) and the mixture stirred at RT for 3 h. The mixture was extracted with EtOAc (3×10 mL), washed with water (10 mL), dried over $MgSO_4$, filtered, and concentrated in vacuo. The crude product was purified by flash column chromatography on silica (EtOAc) to afford **14** as yellow solid (80 mg, 42%). ^{1}H NMR (500 MHz, $CDCl_3$): δ = 9.63 (s, 1H), 7.94 (d, *J* = 1.9 Hz, 1H), 7.72 (dd, *J* = 8.1, 1.9 Hz, 1H), 7.48 (d, *J* = 8.1 Hz, 1H), 6.96 (s, 1H), 2.28 (s, 3H), 1.55 (s, 9H), 1.28 (s, 6H). ^{13}C NMR (126 MHz, $CDCl_3$): δ = 191.29, 167.99, 164.40, 156.95, 146.10, 131.89, 126.89, 121.39, 119.63, 79.69, 54.07, 28.26, 22.93, 15.67; HRMS ESI+ (*m/z*) calcd for $C_{17}H_{23}N_3O_2$: 302.1863 $[M+H]^+$, found: 302.1865.

***tert*-Butyl ((3′,3′-dimethyl-6-nitrospiro[chromene-2,2′-indolin]-5′-yl)(imino)methyl)carbamate (15)**: To a solution of **14** (80 mg, 0.27 mmol) and 2-hydroxy-5-nitrobenzaldehyde (133 mg, 0.80 mmol) in anhydrous ethanol (7 mL) was added TEA (37 μL, 0.27 mmol) and the mixture was heated at reflux under N_2 for 18 h. The volatiles were removed under reduced pressure and the crude product purified by flash column chromatography on silica (1–10% MeOH/$CHCl_3$) to afford **15** as a red solid (43 mg, 36%; 1:2 ratio of SP/MC isomers). ^{1}H NMR (500 MHz, CD_3OD) SP isomer from mixture: δ = 8.13–8.06 (m, 1H), 8.03 (dd, *J* = 8.9, 2.7 Hz, 1H), 7.67–7.62 (m, 2H), 6.96 (d, *J* = 10.3 Hz, 1H), 6.79 (d, *J* = 9.0 Hz, 1H), 6.69 (d, *J* = 8.7 Hz, 1H), 6.08 (d, *J* = 10.3 Hz, 1H), 1.56–1.52 (m, 9H); ^{1}H NMR (500 MHz, CD_3OD) MC isomer from mixture: δ = 8.55 (d, *J* = 2.8 Hz, 1H), 8.13-8.06 (m, 2H), 7.95 (d, *J* = 1.9 Hz, 1H), 7.84 (dd, *J* = 8.1, 1.8 Hz, 1H), 7.60 (d, *J* = 8.1 Hz, 1H), 7.42 (d, *J* = 16.5 Hz, 1H), 6.93 (d, *J* = 9.1 Hz, 1H), 1.56-1.52 (m, 9H); ^{13}C NMR (151 MHz, CD_3OD) mixture of SP and MC signals: δ = 188.76, 169.87, 165.63, 163.74, 157.55, 148.26, 141.13, 136.04, 135.96, 132.97, 132.10, 130.02, 129.27, 127.46, 125.41, 125.37, 125.31, 124.62, 124.60, 123.67, 122.92, 122.69, 122.62, 121.61, 120.76, 117.89, 83.14, 80.97, 62.17, 54.40, 28.48, 24.00, 14.81, 14.62; HRMS ESI+ (*m/z*) calcd for $C_{24}H_{26}N_4O_5$: 451.1976 $[M+H]^+$, found: 451.1976.

3′,3′-Dimethyl-6-nitrospiro[chromene-2,2′-indoline]-5′-carboximidamide (5): Compound **15** (21 mg, 0.05 mmol) was dissolved in 25% TFA/DCM (3 mL) and the mixture stirred at RT for 10 min. The mixture was immediately diluted with DCM (50 mL) and the solvent removed in vacuo. The crude product was purified by RP-HPLC (20-70% MeCN/H_2O) to afford **5** as a yellow solid (4 mg, 25%; 2:1 ratio of SP:MC isomers). ^{1}H NMR (599 MHz, CD_3OD) SP isomer from mixture: δ = 8.13 (d, *J* = 2.7 Hz, 1H), 8.05 (dd, *J* = 9.0, 2.8 Hz, 1H), 7.63 (dd, *J* = 8.3, 2.1 Hz, 1H), 7.59 (d, *J* = 2.0 Hz, 1H), 7 6.99 (d, *J* = 10.3 Hz, 1H), 6.81 (d, *J* = 9.0 Hz, 1H), 6.75 (d, *J* = 8.2 Hz, 1H), 6.09 (d, *J* = 10.2 Hz, 1H), 1.39 (s, 3H), 1.25 (s, 3H); ^{1}H NMR (599 MHz, CD_3OD) MC isomer from mixture: δ = 8.62 (d, *J* = 2.6 Hz, 1H), 8.20–8.15 (m, 2H), 7.92 (d, *J* = 1.9 Hz, 1H), 7.84 (dd, *J* = 8.2, 1.9 Hz, 1H), 7.74 (d, *J* = 8.1 Hz, 1H), .46 (d, *J* = 16.4 Hz, 1H), 7.04 (d, *J* = 9.0 Hz, 1H), 1.57 (s, 3H); ^{13}C NMR (151 MHz, CD_3OD) mixture of SP and MC isomers: δ = 189.86, 168.43, 167.70, 163.55, 159.52, 159.16, 153.52, 148.87, 142.84, 142.22, 138.86, 136.21, 136.15, 130.54, 129.81, 127.93, 127.57, 126.59, 126.45, 125.30, 124.31, 123.71, 123.15, 122.84, 122.73, 121.55, 121.04, 118.52, 117.22, 117.05, 109.27, 54.71, 53.28, 26.32, 23.66, 19.76; HRMS ESI + (*m/z*) calcd for $C_{19}H_{18}N_4O_3$: 351.1452 $[M+H]^+$, found: 351.1453.

3′,3′-Dimethylspiro[chromene-2,2′-indoline]-6-carboximidamide (6): Acetyl chloride (4.8 mL, 68 mmol) was added dropwise to anhydrous ethanol (4.4 mL, 75 mmol) cooled to −78 °C under N_2 and the solution stirred for 5 min. A suspension of 3-formyl-4-hydroxybenzonitrile (100 mg, 0.68 mmol) in EtOAc (5 mL) was then added to the reaction mixture under nitrogen at −78 °C, which was stirred vigorously for a further 10 min. The mixture was warmed to 5 °C and left at 5 °C for 5 days, after which it was warmed to RT and opened to atmosphere. EtOAc (15 mL) was added to the mixture, and the precipitate was collected by suction filtration. The solid was washed with EtOAc (30 mL) and air dried to afford 16 as a pale pink solid (88 mg). The crude product was used in the following reaction without further purification.

7 M ammonia in MeOH (2 mL, 14 mmol) was added dropwise to a vigorously stirring solution of **16** (60 mg, 0.26 mmol) in MeOH (1 mL). The mixture was stirred for 5 days, and then the solvent was removed under reduced pressure to afford crude **17** as a white powder (30 mg) which was used in the following reaction without further purification.

To a solution of **17** (14 mg, 0.09 mmol) in anhydrous ethanol (1 mL) was added 2,3,3-trimethylindolenine (14 μL, 0.09 mmol) and TEA (44 μL, 0.09 mmol). The mixture was heated at reflux under N_2 for 18 h. The solvent was removed in vacuo and the crude product purified by RP-HPLC (20–70% MeCN/H2O) to afford **6** as a yellow solid (1 mg, 4%; 2.5:1 ratio of SP:MC isomers). ^{1}H NMR (599 MHz, CD_3OD) SP isomer from mixture: δ = 7.66 (d, *J* = 2.5 Hz, 1H), 7.60-7.54 (m, 1H), 7.11-7.02 (m, 2H), 6.90 (d, *J* = 10.4 Hz, 1H), 6.86 (d, *J* = 8.6 Hz, 1H), 6.81 (td, *J* = 7.4, 1.0 Hz, 1H), 6.66 (d, *J* = 7.7 Hz, 1H), 6.07 (d, *J* = 10.4 Hz, 1H), 1.24 (s, 6H);

^{1}H NMR (599 MHz, CD_3OD) MC isomer from mixture: $\delta = 8.21$ (d, $J = 2.5$ Hz, 1H), 8.09 (d, $J = 16.6$ Hz, 1H), 7.72 (dd, $J = 8.6$, 2.4 Hz, 1H), 7.60-7.54 (m, 1H), 7.48 (d, $J = 7.4$ Hz, 1H), 7.42 (d, $J = 16.7$ Hz, 1H), 7.39 (td, $J = 7.7$, 0.9 Hz, 1H), 7.33 (td, $J = 7.4$, 1.0 Hz, 1H), 7.11-7.02 (m, 1H), 1.54 (s, 6H); ^{13}C NMR (151 MHz, CD_3OD) mixture of SP and MC isomers: $\delta = 186.12$, 171.61, 167.49, 162.81, 158.99, 143.88, 142.37, 131.75, 130.51, 129.69, 129.29, 128.57, 128.15, 127.90, 124.01, 122.90, 122.83, 121.01, 120.49, 120.26, 117.68, 117.46, 24.31; HRMS ESI+ (*m/z*) calcd for $C_{19}H_{19}N_3O$: 306.1601 [$M + H$]$^+$, found: 306.1603.

General synthesis of linear peptides by SPPS: 2-Chlorotrityl chloride functionalised polystyrene resin (Chem Impex Intl. Ltd., 1.4 mmol g^{-1}, 1.0 g) was allowed to swell for 15 min in DCM (15 mL). Fmoc-Ser(*t*Bu)-OH (1.0 mmol) was dissolved in DCM (10 mL) and added to the swollen resin, followed by DIPEA (5.0 mmol) and the mixture agitated for 2 h. MeOH (5 mL) was then added to the mixture which was agitated for a further 10 min. The solution was drained from the resin, and the resin was subsequently washed with DCM (5×10 mL) and diethyl ether (5×10 mL) and left to air dry overnight and the loading of the Fmoc-Ser(*t*Bu)-OH determined by a weight increase.

A portion of the FmocAA functionalised resin (0.25 mmol) was pre-swelled in a solution of 1:1 DCM/DMF (10 mL) for 15 min, then the solution drained from the resin. The Fmoc protecting group was then deprotected by addition of a 20% solution of piperidine in DMF with 0.1 M HOBt (5 mL) to the resin, and stirred intermittently for 15 min. The solution was drained from the resin in vacuo, and the resin was then washed with DMF (5×10 mL), DCM (5×10 mL) and DMF (5×10 mL). Amino acid coupling was achieved by addition of a solution of FmocAA (or FmocAzo-OH) (5 equiv.) with 0.5 M solution of HATU in DMF (2.5 mL, 5 equiv.), DIPEA (435 μL, 10 equiv.) and DMF (8 mL). The mixture was added to the resin and left for 2 h, with intermittent stirring. The solution was drained from the resin in vacuo and washed with DMF (5×10 mL), DCM (5×10 mL) and DMF (5×10 mL). In the case of coupling Fmoc-Pro-OH, or coupling the residue subsequent (N-terminal) to a proline residue, the coupling was repeated once more ("double coupling"), prior to Fmoc deprotection, to ensure complete acylation. Coupling/deprotection steps were repeated to elongate the peptide.

The TNBS test for a free amine was employed after coupling and deprotection steps to ensure the completion of the reaction, indicated by colourless resin beads. This was performed via addition of a 20% *v/v* solution of 5% aqueous TNBS in DMF (50 μL), and a 5% solution of DIPEA in DMF (50 μL) to a small amount of resin (micro spatula-full). The mixture was shaken for 1 minute to allow for reaction. Red beads indicated the presence of free (primary) amine, and colourless beads indicated the absence of free amines. If the coupling or deprotection reaction was not complete, then the step was repeated, including the TNBS test for a free amine. Once the desired sequence was achieved, and the final Fmoc group was deprotected, the resin was washed with DMF (5×10 mL), DCM (5×10 mL) and diethyl ether (5×10 mL). The remaining ether was left to evaporate overnight. The peptide chain was cleaved from the resin by addition of a solution of 1% TFA in DCM (10 mL) and agitation for 1 h. The mixture was filtered (glass sinter) and the TFA solution retained. Fresh cleavage solution was added to the resin, and the reaction repeated for a further 1 h. The combined solutions were concentrated under nitrogen to approx. 1 mL volume, to which diethyl ether (10 mL) was added and the mixture was kept at 4 °C overnight. The mixture was subsequently centrifuged, and the supernatant decanted from the precipitate, and the precipitate dried under nitrogen. The dried solid was then dissolved in 30% aqueous MeOH (~5 mg mL^{-1}) and lyophilised to give the crude product as an orange/brown solid.

General synthesis for peptide cyclisation: Crude linear peptide (~2 mg mL^{-1} in DMF) was converted to the *cis* geometry by irradiation for 18 h with UV light (352 nm), in a quartz flask. A solution of HATU (3 equiv.), HOAt (3 equiv.) and in DMF with 1% DIPEA (final peptide conc. of 1 mg mL^{-1}) was added to the peptide and the resulting mixture stirred under UV irradiation (352 nm) for 18 h or until cyclisation was complete as indicated by HPLC and MS. The mixture was concentrated in vacuo, taken up in DCM (15 mL) and washed successively with 1 M HCl (15 mL), saturated aqueous $NaHCO_3$ (15 mL) and brine (15 mL). The organic layer was concentrated in vacuo and the residue added to a solution of 1:1 TFA/DCM with 2.5% each TIPS and H_2O (10 mL) and stirred for 2 h. The mixture was concentrated under a stream of nitrogen to ~1 mL, then the peptide precipitated by addition of diethyl ether (10 mL) and the mixture chilled at 4 °C overnight. The mixture was subsequently centrifuged, and the supernatant decanted from the precipitate, and the precipitate dried under nitrogen. The dried solid was then dissolved in 30% aqueous MeOH (~5 mg mL^{-1}) and purified by RP-HPLC to yield the cyclic peptides.

In solution photoswitching: A stock solution of each photoswitchable small molecule/peptide was made up at 10 mM in DMSO. These stocks were then diluted to 200 μM in DMSO and Tris buffer + 2% DMSO in a 96-well, clear bottom plate for switching experiments using a Synergy H4 Microplate Reader. For all compounds an absorption spectrum was taken under visible light ("before irradiation") and after irradiation with UV light (352 nm) for 15 min ("after irradiation"). For spiropyrans **1**, **2**, **5** and **6**, a fluorescence emission spectrum was also taken ($\lambda_{ex} = 532$ nm) before and after irradiation. These spectra look distinctly different for each isomer (SP/MC and *trans/cis*) and so provide qualitive information on whether switching between isomers has occurred. Experiments were performed in triplicate.

Furthermore, for all compounds except **1** and **2**, NMR spectra were used to quantify the composition of the TAS and PSS. Samples were dissolved in CD_3OD in a quartz NMR tube, and a spectrum under visible light was taken. Each sample was irradiated with UV light (352 nm) in the quartz tube for 1 h, and a further NMR spectrum taken. Integration of aromatic peaks corresponding to each isomer in each spectrum was used to determine the TAS/PSS ratios.

In vitro trypsin assay: Fluorometric trypsin assays were carried out on a Synergy H4 hybrid reader at 25 ± 0.4 °C using 96-well, clear bottom plates. Tris buffer was made up containing 100 mM Trizma base with 10 mM $CaCl_2$ at pH 7.8 and kept at 4 °C until needed, when it was warmed to RT. Trypsin from bovine pancreas was dissolved daily in 1 mM HCl (0.1 mg mL^{-1}) and kept at 0 °C. A 1 μg mL^{-1} solution of trypsin was prepared freshly before each experiment by diluting the 0.1 mg mL^{-1} solution into Tris buffer. The substrate Boc-Phe-Ser-Arg-AMC (Bachem, USA) was dissolved in DMSO (40 mM) and stored at −20 °C until needed, when it was diluted to 1 mM in Tris buffer before each experiment. 10 mM stock solutions (DMSO) of each inhibitor were diluted in DMSO to the concentration required for addition to the plate. Each inhibitor was tested at 6 different concentrations [I], which were varied based on the predicted activity of each compound (see plots in Figures S13 and S14).

For the assays under visible light (TAS), 85 μL of Tris buffer was added to each well, followed by 2.5 μL of Boc-Phe-Ser-Arg-AMC and 2.5 μL of inhibitor at each concentration. Finally, 10 μL of trypsin was added to each well, making up a total volume of

100 μL (2.5% DMSO), and each well was mixed, and the plate then read. For the irradiated assays (PSS), inhibitors were first diluted in a 96-well plate, in 50:50 DMSO/Tris buffer. This plate was then irradiated under UV light (352 nm), for 30 min for the small-molecule inhibitors, and 1 h for the peptide inhibitors. The rest of the assay was subsequently carried out in dark conditions. 82.5 μL Tris buffer, 2.5 μL of substrate, 5 μL inhibitor and 10 μL enzyme were added to the plate, and the wells were then mixed and read. A positive control containing 95 μL Tris buffer plus 2.5 μL substrate and 2.5 μL DMSO was also run for each compound. Fluorescence emission (440 nm) was recorded every 30 s for 8 min, with excitation at 360 nm. Experiments were performed in triplicate.

The rate of enzyme-catalysed hydrolysis of Boc-Phe-Ser-Arg-AMC was calculated for the positive control (no inhibitor) and set as 100%. The rate of reaction for each inhibitor concentration was then calculated and normalised as a % of this positive control. Log[I] against v[%] was plotted by using GraphPad Prism 9, which generated IC_{50} values for each inhibitor. These IC_{50} values were then used to calculate K_i values for the inhibitors by using Equation (1):[29]

$$K_i = \frac{IC_{50}}{\left(1+\frac{[S]}{K_m}\right)} \quad (1)$$

Where [S] is 25 μM and $K_m = 19$ μM (determined experimentally).

In silico docking: Docking experiments were performed using ICM software version 3.8-6 (Molsoft L.L.C., San Diego, CA, USA). The protein for docking was retrieved from PSCB protein data bank 3ATL.[30] Then, formal charges were assigned; protonation states of histidines were adjusted, and hydrogens, histidine, glutamine, and asparagine were optimised using the protein preparation procedure implemented in ICM.[35] The original bound ligand and all water molecules were removed from the binding site before docking. The binding site was defined as the cavity delimited by residues with at least one nonhydrogen atom within a 4.0 Å cut-off radius from the ligand **4**. The pocket was represented by 0.5 Å grid maps accounting for hydrogen bonding, hydrophobic, van der Waals, and electrostatic interactions. The molecules were flexibly docked into the rigid binding site and scored based on the ICM scoring function.

Molecular modelling: The lowest-energy structures for the *trans* and *cis* isomers of **p2** and **p3** were determined in the gas phase, using the NWChem 6.6 package[34] with tight convergent criteria and using a hybrid B3LYP functional with 6-31G basis set for all atoms. The structures were visualised using Discovery Studio software (Dassault Systemes BIOVIA, Paris, France).

Supporting Information

Additional references are cited in the Supporting Information.[36–39]

Acknowledgements

This work was supported by the Australian Research Council (ARC) Centre of Excellence for Nanoscale Biophotonics (CE140100003). We also acknowledge the Australian National Fabrication Facility for providing the analytical facilities used in this work. The computational aspects of this work were supported by an award under the National Computational Merit Allocation Scheme for J.Y. on the National Computing Infrastructure (NCI) National Facility at the Australian National University. The authors would also like to acknowledge Aimee Horsfall, Sabrina Heng, Kwang Jun Lee, Andrew Marshall and Robert McLaughlin for their contributions to this work. Open Access publishing facilitated by The University of Adelaide, as part of the Wiley - The University of Adelaide agreement via the Council of Australian University Librarians.

Conflict of Interests

The authors declare no conflict of interest.

Data Availability Statement

The data that support the findings of this study are available from the corresponding author upon reasonable request.

Keywords: enzymes · peptides · photochemistry · photoswitches · trypsin

[1] N. C. Nicolaides, P. M. Sass, L. Grasso, *Expert Opin. Drug Discovery* **2010**, *5*, 1123–1140.
[2] W. A. Velema, W. Szymanski, B. L. Feringa, *J. Am. Chem. Soc.* **2014**, *136*, 2178–2191.
[3] R. Langer, *Nature* **1998**, *392*, 5–10.
[4] G. Wu, T. Zhao, D. Kang, J. Zhang, Y. Song, V. Namasivayam, J. Kongsted, C. Pannecouque, E. De Clercq, V. Poongavanam, X. Liu, P. Zhan, *J. Med. Chem.* **2019**, *62*, 9375–9414.
[5] J. Broichhagen, J. A. Frank, D. Trauner, *Acc. Chem. Res.* **2015**, *48*, 1947–1960.
[6] M. M. Lerch, M. J. Hansen, G. M. VanDam, W. Szymanski, B. L. Feringa, *Angew. Chem. Int. Ed.* **2016**, *55*, 2–24.
[7] J. A. Frank, M. Moroni, R. Moshourab, M. Sumser, G. R. Lewin, D. Trauner, *Nat. Commun.* **2015**, *6*, 71118.
[8] J. Broichhagen, N. R. Johnston, Y. Von Ohlen, H. Meyer-Berg, B. J. Jones, S. R. Bloom, G. A. Rutter, D. Trauner, D. J. Hodson, *Angew. Chem. Int. Ed.* **2016**, *55*, 5865–5868.
[9] J. Broichhagen, I. Jurastow, K. Iwan, W. Kummer, D. Trauner, *Angew. Chem. Int. Ed.* **2014**, *53*, 7657–7660.
[10] M. Borowiak, W. Nahaboo, M. Reynders, K. Nekolla, P. Jalinot, J. Hasserodt, M. Rehberg, M. Delattre, S. Zahler, A. Vollmar, D. Trauner, O. Thorn-Seshold, *Cell* **2015**, *162*, 402–411.
[11] B. Blanco, K. A. Palasis, A. Adwal, D. F. Callen, A. D. Abell, *Bioorg. Med. Chem.* **2017**, *25*, 5050–5054.
[12] W. A. Velema, J. P. Van Der Berg, M. J. Hansen, W. Szymanski, A. J. M. Driessen, B. L. Feringa, *Nat. Chem.* **2013**, *5*, 924–928.
[13] K. Hüll, J. Morstein, D. Trauner, *Chem. Rev.* **2018**, *118*, 10710–10747.
[14] K. A. Palasis, N. A. Lokman, B. C. Quirk, A. Adwal, L. Scolaro, W. Huang, C. Ricciardelli, M. K. Oehler, R. A. McLaughlin, A. D. Abell, *Int. J. Mol. Sci.* **2021**, *22*, 10844.
[15] P. Kobauri, F. J. Dekker, W. Szymanski, B. L. Feringa, *Angew. Chem. Int. Ed.* **2023**, *62*, e202300681.
[16] "Kiora's Investigational Treatment for Retinitis Pigmentosa, KIO-301, Demonstrates Visual Function Restoration in Patients Who Are Blind," can be found under https://ir.kiorapharma.com/news-events/press-releases/detail/179/kioras-investigational-treatment-for-retinitis-pigmentosa, **2023**.
[17] H. D. Bartunik, L. J. Summers, H. H. Bartsch, *J. Mol. Biol.* **1989**, *210*, 813–828.
[18] L. Hedstrom, *Chem. Rev.* **2002**, *102*, 4501–4523.

[19] K. Tanizawa, S. Ishii, K. Hamaguchi, Y. Kanaoka, *J. Biochem.* **1971**, *69*, 893–899.
[20] B. A. Katz, K. Elrod, E. Verner, R. L. Mackman, C. Luong, W. D. Shrader, M. Sendzik, J. R. Spencer, P. A. Sprengeler, A. Kolesnikov, V. W. F. Tai, H. C. Hui, J. G. Breitenbucher, D. Allen, J. W. Janc, *J. Mol. Biol.* **2003**, *329*, 93–120.
[21] A. Gitlin-Domagalska, A. Maciejewska, D. Dębowski, *Pharmaceuticals* **2020**, *13*, 1–40.
[22] S. J. de Veer, A. M. White, D. J. Craik, *Angew. Chem. Int. Ed.* **2021**, *60*, 8050–8071.
[23] R. Klajn, *Chem. Soc. Rev.* **2014**, *43*, 148–184.
[24] A. A. Beharry, G. A. Woolley, *Chem. Soc. Rev.* **2011**, *40*, 4422–4437.
[25] A. Descours, K. Moehle, A. Renard, J. A. Robinson, *ChemBioChem* **2002**, *3*, 318–323.
[26] X. Zhang, S. Heng, A. D. Abell, *Chem. Eur. J.* **2015**, *21*, 10703–10713.
[27] E. Verner, B. A. Katz, J. R. Spencer, D. Allen, J. Hataye, W. Hruzewicz, H. C. Hui, A. Kolesnikov, Y. Li, C. Luong, A. Martelli, K. Radika, R. Rai, M. She, W. Shrader, P. A. Sprengeler, S. Trapp, J. Wang, W. B. Young, R. L. Mackman, *J. Med. Chem.* **2001**, *44*, 2753–2771.
[28] A. Nudelman, Y. Bechor, E. Falb, B. Fischer, B. A. Wexler, A. Nudelman, *Synth. Commun.* **1998**, *28*, 471–474.
[29] C. Yung-Chi, W. H. Prusoff, *Biochem. Pharmacol.* **1973**, *22*, 3099–3108.
[30] J. Yamane, M. Yao, Y. Zhou, Y. Hiramatsu, K. Fujiwara, T. Yamaguchi, H. Yamaguchi, H. Togame, H. Tsujishita, H. Takemoto, I. Tanaka, *J. Appl. Crystallogr.* **2011**, *44*, 798–804.
[31] O. Babii, S. Afonin, C. Diel, M. Huhn, J. Dommermuth, T. Schober, S. Koniev, A. Hrebonkin, A. Nesterov-Mueller, I. V. Komarov, A. S. Ulrich, *Angew. Chem. Int. Ed.* **2021**, *60*, 21789–21794.
[32] T. Podewin, M. S. Rampp, I. Turkanovic, K. L. Karaghiosoff, W. Zinth, A. Hoffmann-Röder, *Chem. Commun.* **2015**, *51*, 4001–4004.
[33] K. Rück-Braun, S. Kempa, B. Priewisch, A. Richter, S. Seedorff, L. Wallach, *Synthesis (Stuttg).* **2009**, 4256–4267.
[34] M. Valiev, E. J. Bylaska, N. Govind, K. Kowalski, T. P. Straatsma, H. J. J. Van Dam, D. Wang, J. Nieplocha, E. Apra, T. L. Windus, W. A. De Jong, *Comput. Phys. Commun.* **2010**, *181*, 1477–1489.
[35] M. A. C. Neves, M. Totrov, R. Abagyan, *J. Comput.-Aided Mol. Des.* **2012**, *26*, 675–686.
[36] G. M. Sylvia, S. Heng, A. Bachhuka, H. Ebendorff-Heidepriem, A. D. Abell, *Tetrahedron* **2018**, *74*, 1240–1244.
[37] H. Görner, *Phys. Chem. Chem. Phys.* **2001**, *3*, 416–423.
[38] H. M. D. Bandara, S. C. Burdette, *Chem. Soc. Rev.* **2012**, *41*, 1809–25.
[39] M. Hammarson, J. R. Nilsson, S. Li, P. Lincoln, J. Andréasson, *Chem. Eur. J.* **2014**, *20*, 15855–15862.

Manuscript received: June 18, 2023
Revised manuscript received: August 13, 2023
Accepted manuscript online: August 16, 2023
Version of record online: September 4, 2023